

SUPPLEMENTARY DATA

A protein-based electrochemical biosensor for detection of tau protein, a neurodegenerative disease biomarker

Jose O. Esteves-Villanueva, Hanna Trzeciakiewicz, Sanela Martić*

Department of Chemistry, Oakland University, 2200 North Squirrel Road, Rochester, MI, 48309, USA; martic@oakland.edu

Corresponding author: Sanela Martic, Department of Chemistry, Oakland University, 2200 North Squirrel Road, Rochester, MI, 48309, USA, martic@oakland.edu, [Tel:1-248-370-3088](tel:1-248-370-3088); Fax: 1-248-370-2321.

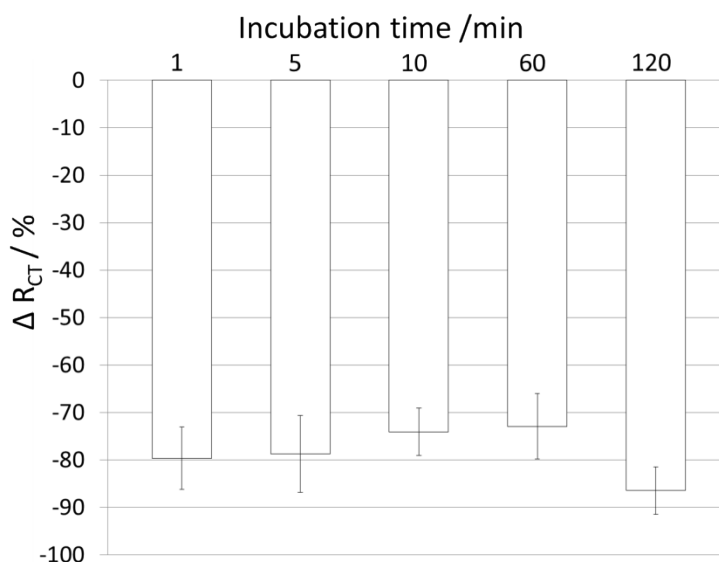


Fig. S1. Plot of % ΔR_{ct} as a function of incubation time of tau-Au surface into solution tau at 5 μM .

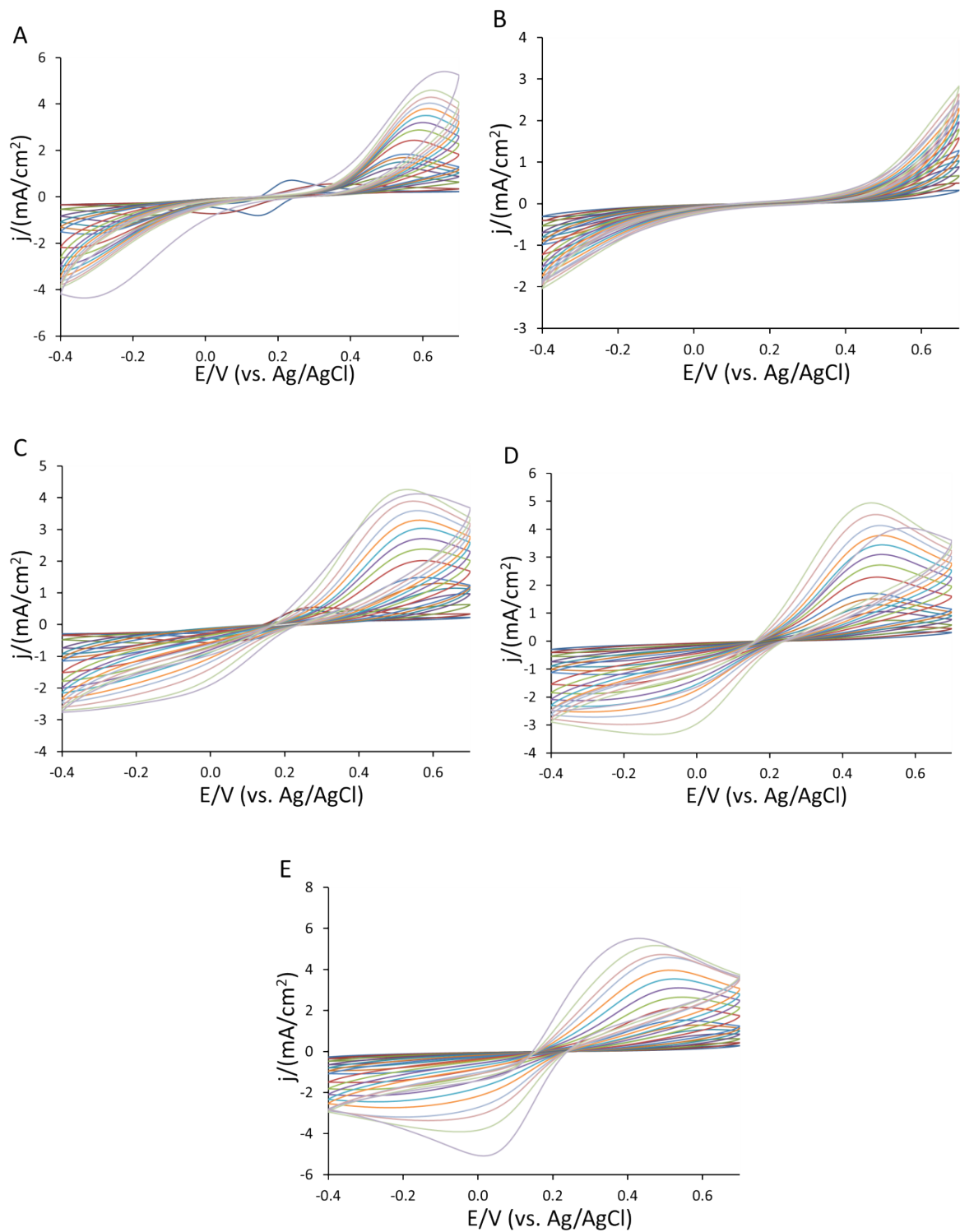


Fig. S2. CVs versus scan rates for Lip-NHS (A), tau-Au (B), ethanolamine-tau-Au (C), hexanethiol-ethanolamine-tau-Au (D), and tau-tau-Au (E) (10 mM phosphate buffer, pH 6.8, 10 mM $[\text{Fe}(\text{CN})_6]^{3-/4-}$).

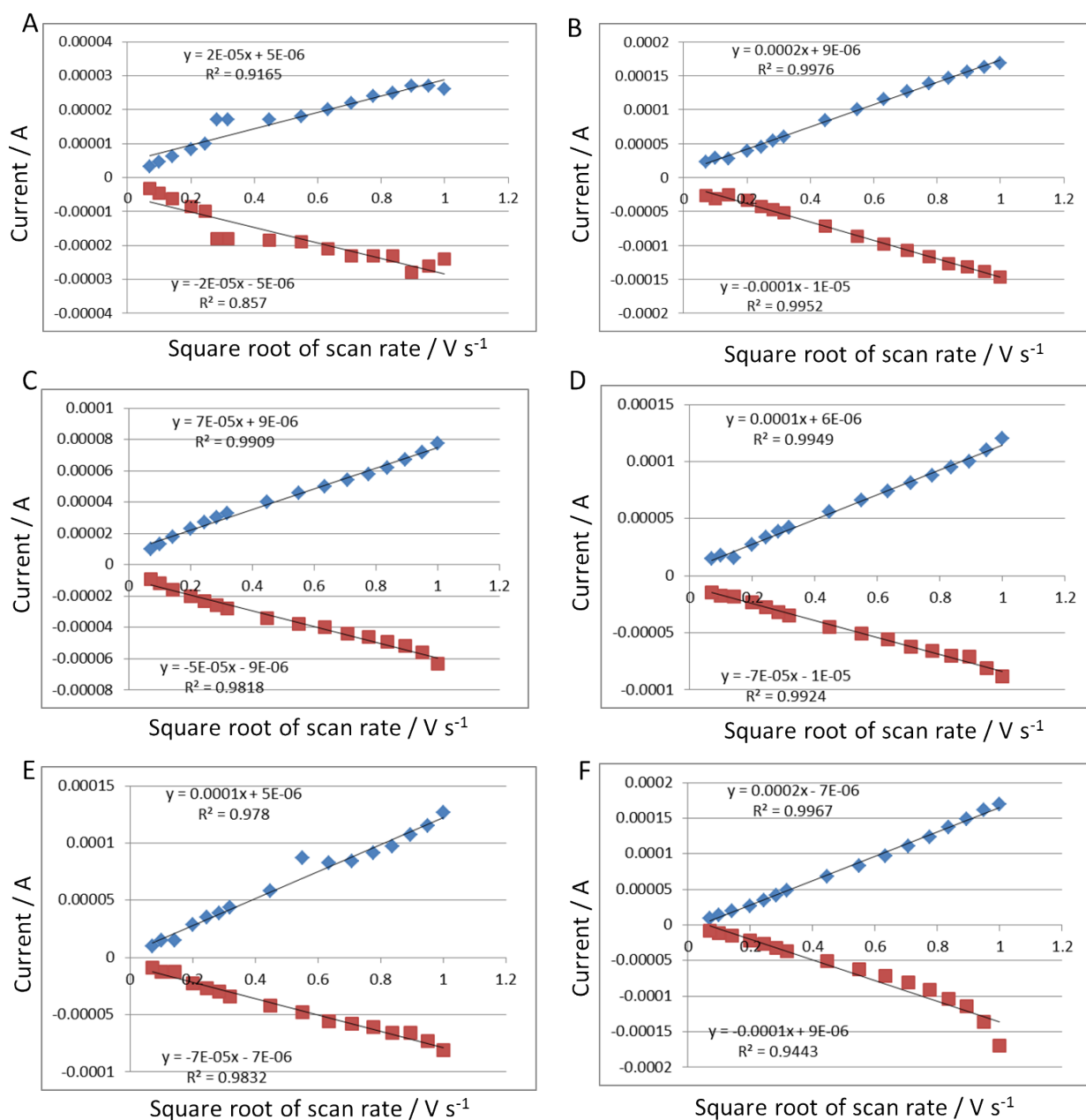


Fig. S3. Plots of current density as a function of scan rate (5 mV to 1000 mV) for stepwise modification: a) bare Au, b) Lip-NHS, c) tau, d) ethanolamine, and e) hexanethiol (tau-Au). F) The tau-Au surfaces was exposed to solution tau to fabricate tau-tau-Au surface (f) (10 mM [Fe(CN)₆]^{3-/4-} in 10 mM phosphate buffer, pH 6.8).

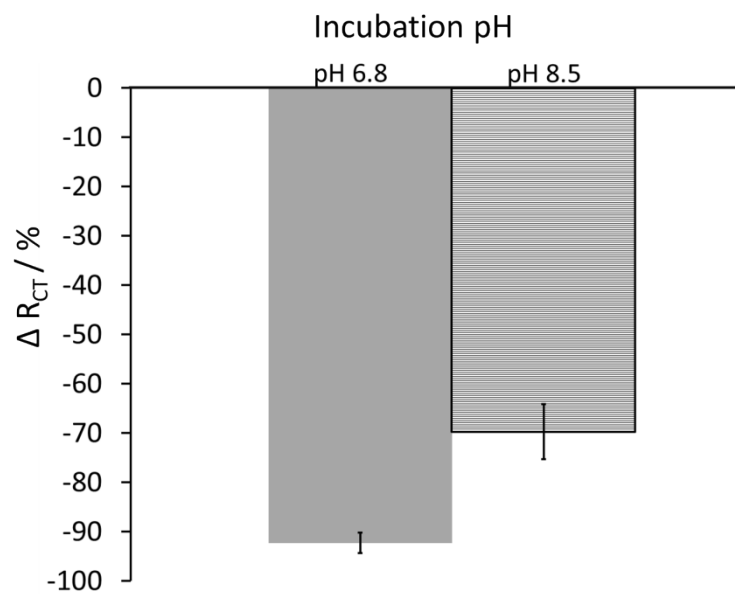


Fig. S4. Plot of $\% \Delta R_{ct}$ as a function of incubation pH between solution tau and tau-Au surface.

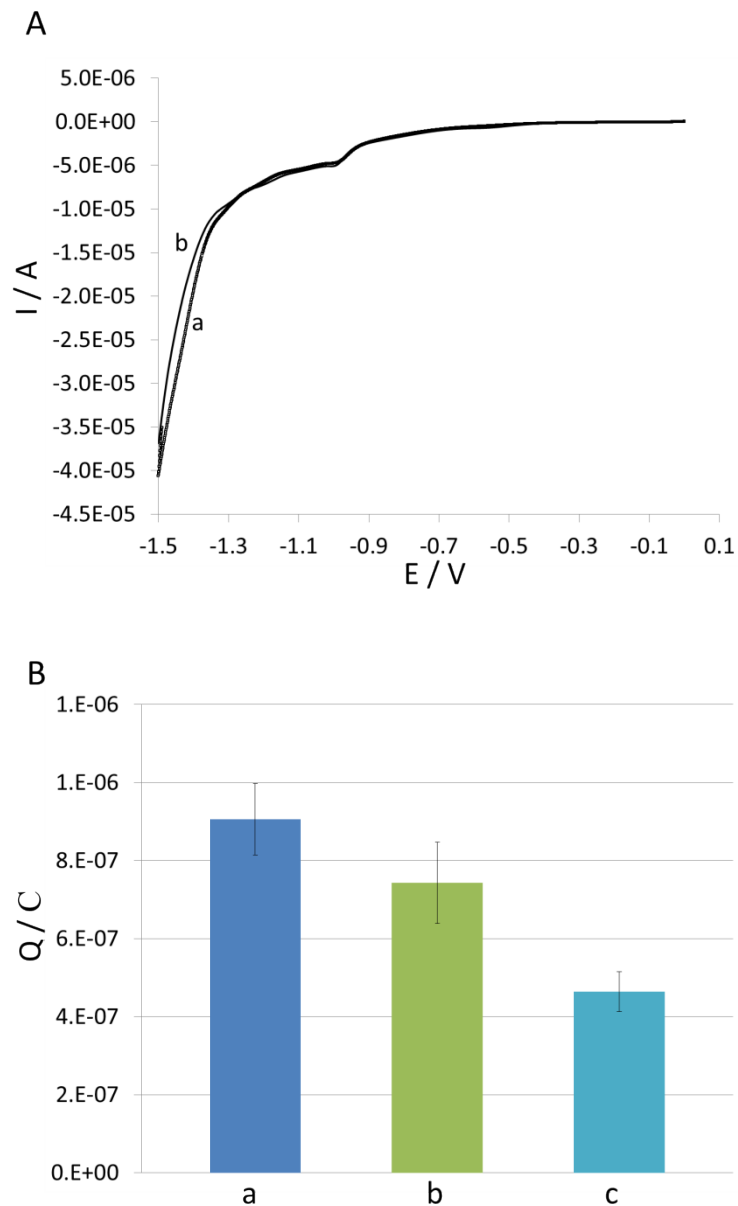


Fig. S5. (A) Cyclic voltammogram segments of tau-Au (a) and tau-tau-Au (b) (0.5 M KOH, 100 mV s^{-1} scan rate). (B) Plot of charge as a function of film type: tau-Au (a), tau-tau-Au (b) and bare Au (c). The charge was determined from reductive cyclic voltammograms in (A); error bars represent triplicate measurements.

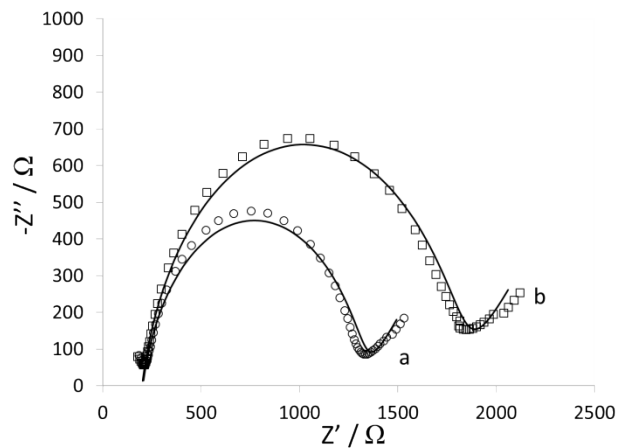


Fig. S6. Nyquist plots of tau films before (a) and after (b) incubation in buffer (10 mM phosphate buffer pH 6.8, 10 mM $[\text{Fe}(\text{CN})_6]^{3-/4-}$, tau-modified Au working electrode, Pt-wire auxiliary electrode and Ag/AgCl reference electrode). Computational settings were: 5 mV amplitude, 1 Hz to 100 kHz range, and open circuit potential.

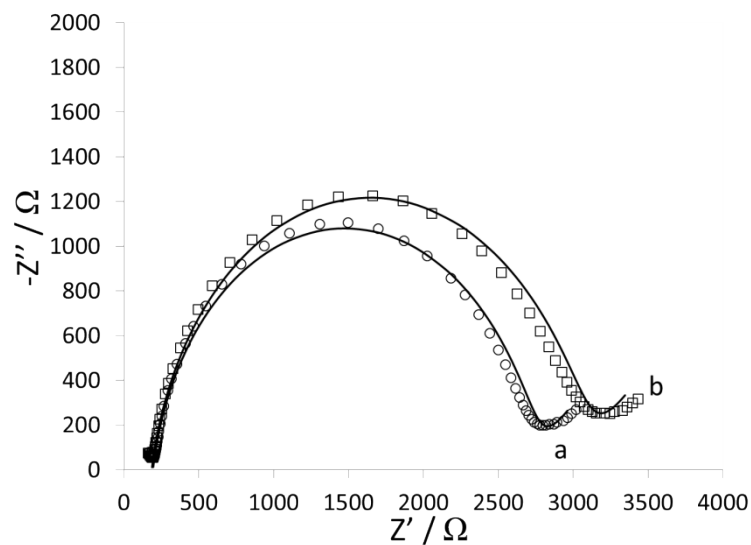


Fig. S7. Nyquist plots of tau films before (a) and after (b) incubation in 5 μM BSA solution (10 mM phosphate buffer pH 6.8, 10 mM $[\text{Fe}(\text{CN})_6]^{3-/4-}$, tau-modified Au working electrode, Pt-wire auxiliary electrode and Ag/AgCl reference electrode). Computational settings were: 5 mV amplitude, 1 Hz to 100 kHz range, and open circuit potential.

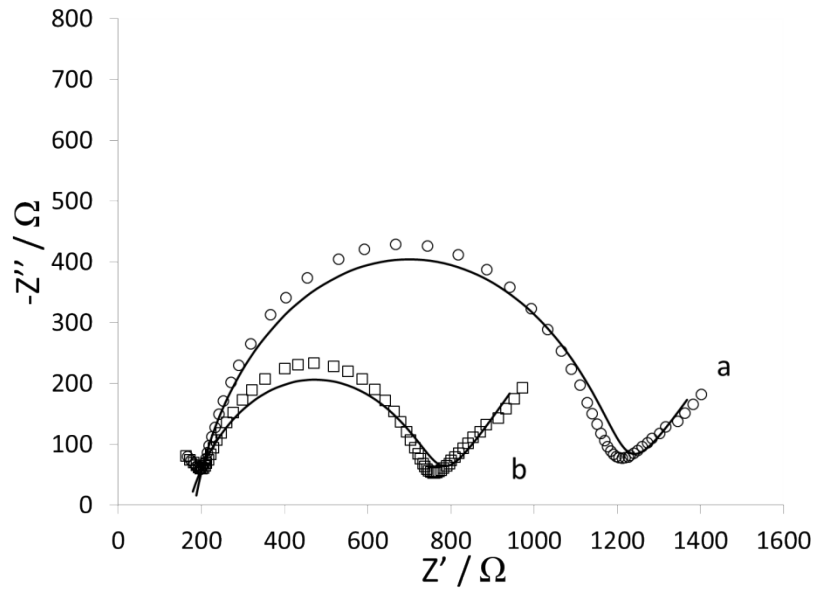


Fig. S8. Nyquist plots of tau-free films (prepared by omitting the immobilization of tau step during surface modifications), before (a) and after (b) incubation in 5 μM tau solution (10 mM phosphate buffer pH 6.8, 10 mM $[\text{Fe}(\text{CN})_6]^{3-/4-}$, tau-modified Au working electrode, Pt-wire auxiliary electrode and Ag/AgCl reference electrode). Computational settings were: 5 mV amplitude, 1 Hz to 100 kHz range, and open circuit potential.

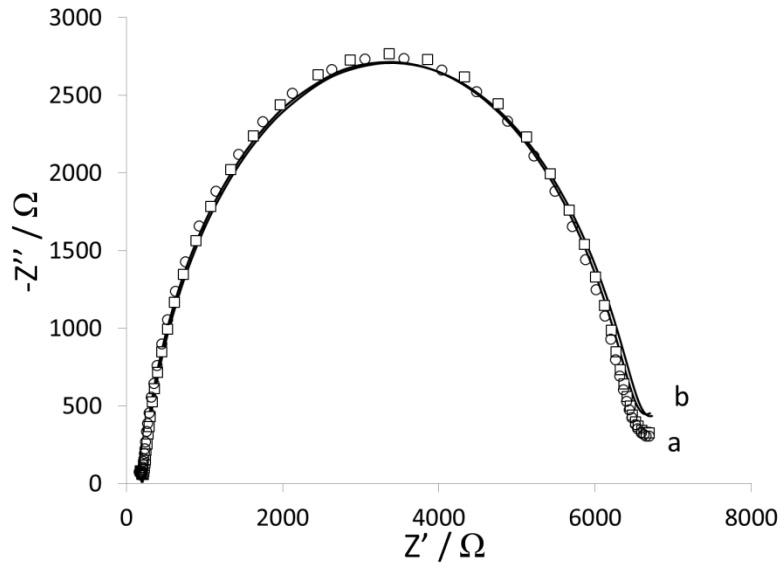


Fig. S9. Nyquist plots of tau films before (a) and after (b) incubation in 0.2 μM tau solution (10 mM phosphate buffer pH 6.8, 10 mM $[\text{Fe}(\text{CN})_6]^{3-/4-}$, tau-modified Au working electrode, Pt-wire auxiliary electrode and Ag/AgCl reference electrode). Computational settings were: 5 mV amplitude, 1 Hz to 100 kHz range, and open circuit potential.

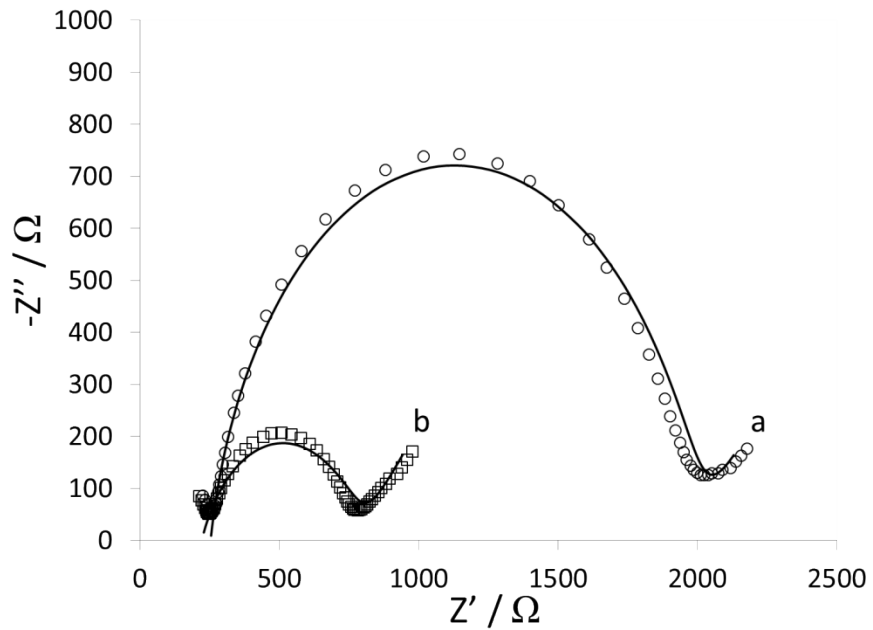


Fig. S10. Nyquist plots of tau films before (a) and after (b) incubation in 5 μM tau solution at pH 8.5 (10 mM phosphate buffer pH 6.8, 10 mM $[\text{Fe}(\text{CN})_6]^{3-/4-}$, tau-modified Au working electrode, Pt-wire auxiliary electrode and Ag/AgCl reference electrode). Computational settings were: 5 mV amplitude, 1 Hz to 100 kHz range, and open circuit potential.

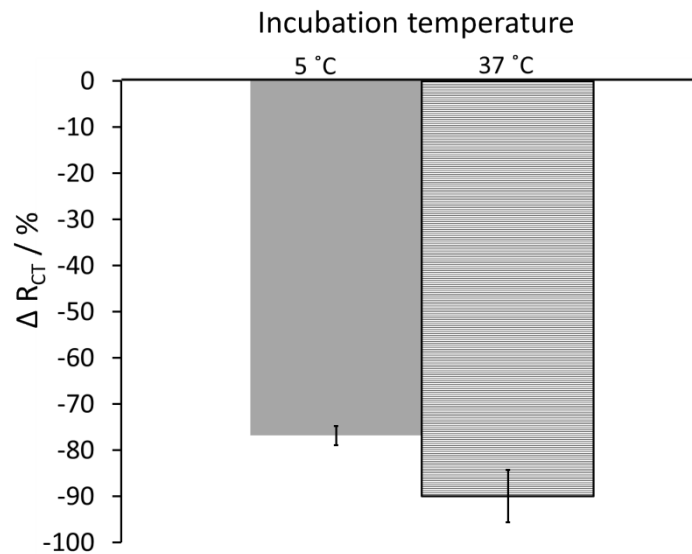


Fig. S11. Plot of charge transfer resistance as a function of temperature during incubation of tau film in 5 μM tau solution: 5 ° and 37 °C (10 mM phosphate buffer pH 6.8, 10 mM $[\text{Fe}(\text{CN})_6]^{3-/4-}$, tau-modified Au working electrode, Pt-wire auxiliary electrode and Ag/AgCl reference electrode).

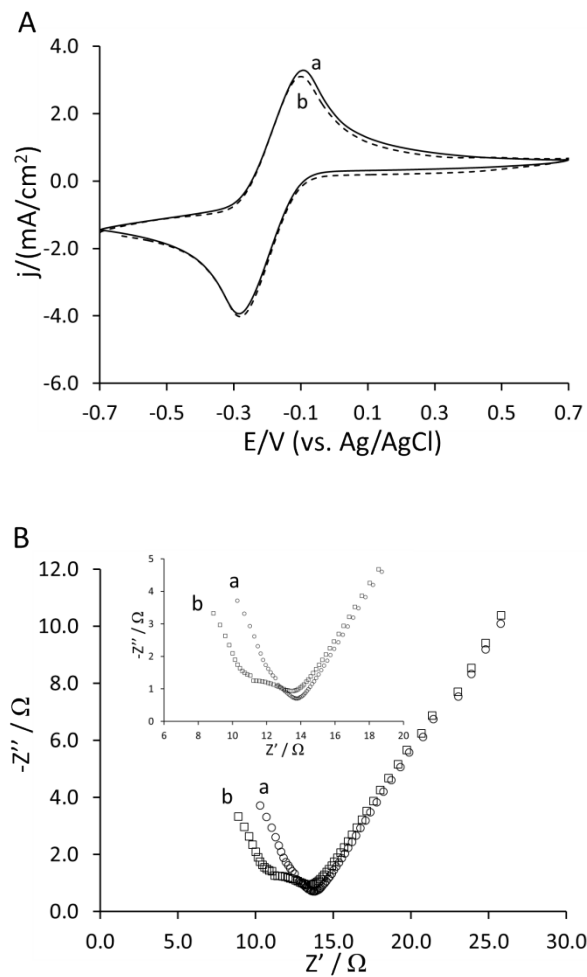


Fig. S12. (A) CV and (B) EIS of tau-Au (a) and tau-tau-Au (b) (10 mM phosphate buffer pH 6.8, 10 mM $[\text{Ru}(\text{NH}_3)_6]^{2+/3+}$, tau-modified Au working electrode, Pt-wire auxiliary electrode and Ag/AgCl reference electrode). Computational settings were: 100 mV s⁻¹ scan rate, 5 mV amplitude, 1 Hz to 100 kHz range, and open circuit potential.

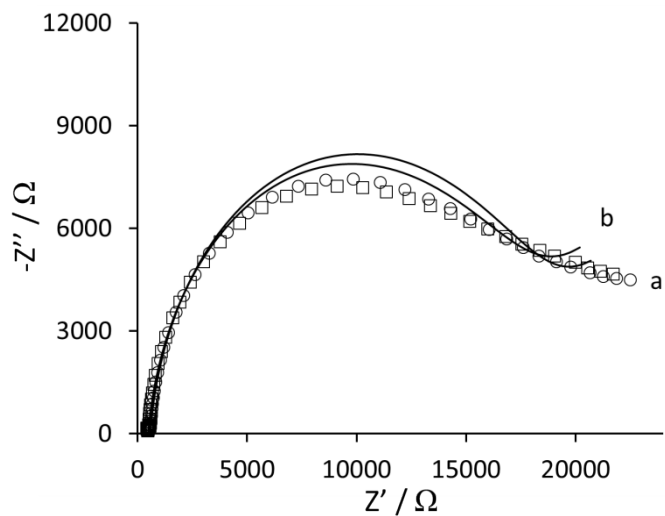


Fig. S13. Nyquist plots of tau films before (a) and after (b) incubation in 250 $\mu\text{g/mL}$ PHF solution at pH 7.4 (10 mM phosphate buffer pH 6.8, 10 mM $[\text{Fe}(\text{CN})_6]^{3-/4-}$, tau-modified Au working electrode, Pt-wire auxiliary electrode and Ag/AgCl reference electrode). Computational settings were: 5 mV amplitude, 1 Hz to 100 kHz range, and open circuit potential.

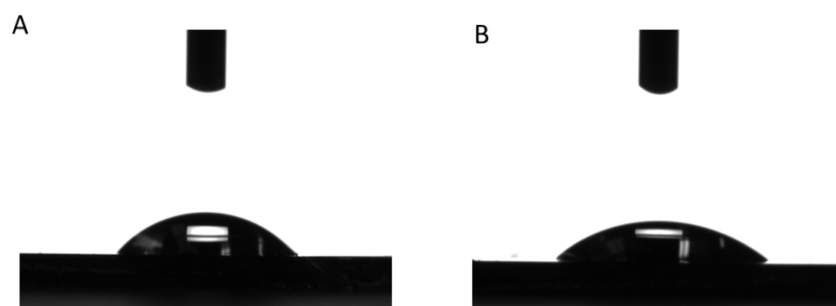


Fig. S14. Contact angle images of tau-Au (A) and tau-tau-Au (B) (solution tau at 5 μ M, 10 mM phosphate buffer, pH 6.8).

Table S1. Static buffer contact angle (θ (deg)) and the ellipsometric parameter thickness (d (nm)) of the tau film before and after incubation in tau solution.

Film Type	d / nm	Θ / °(deg)
Tau-Au	8.4 ± 5	47 ± 4
Tau-tau-Au	8.1 ± 1	40 ± 2